Case Study: Myoglobin

Anton Arkhipov, Rosemary Braun and Ying Yin

December 12, 2005

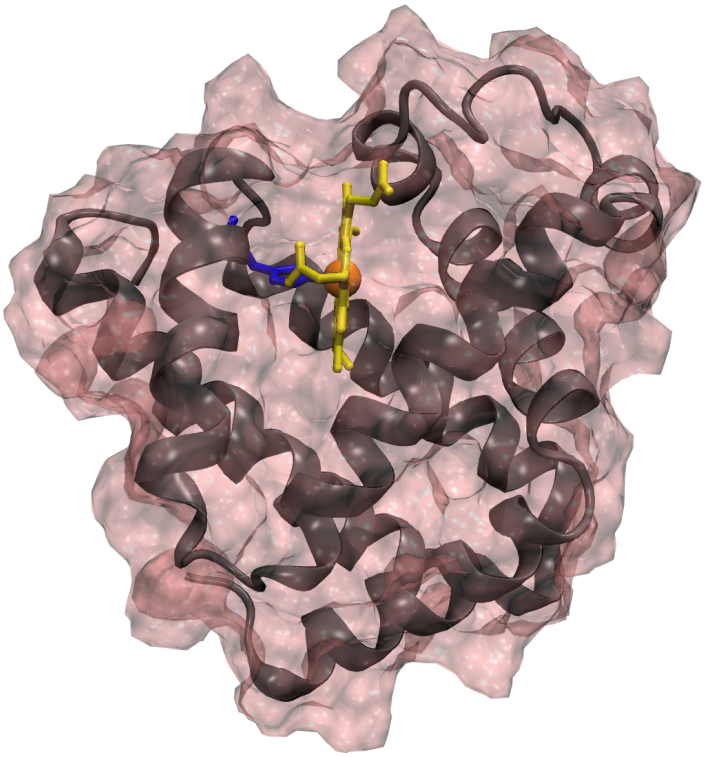

Introduction

Myoglobin is a small, monomeric protein which serves as an intracellular oxygen storage site. It is found in abundance in the skeletal muscle of vertebrates, and is responsible for the characteristic red color of muscle tissue. Myoglobin is closely related to hemoglobin, which consists of four myoglobin-like subunits that form a tetramer and are responsible for carrying oxygen in blood. In humans, blood-borne cardiac myoglobin can serve as a biomarker of heart attack, since blood myoglobin levels rise in two to three hours following muscle injury.

The atomic structure of myoglobin has been known since 1957, when John Kendrew demonstrated that X-ray crystallography can reveal the structure of entire proteins [1, 2]. Myoglobin stands out as the first structurally determined protein, and has been the subject of many detailed studies by a large number of experimental and computational methods (*e. g.*, [3, 4, 5, 6, 7, 8, 9, 10, 11, 12, 13]) because of its ability to bind oxygen reversibly. The oxygen-binding capability of myoglobin is conferred by a heme prosthetic group which sits in a cleft of the myoglobin molecule. The structure and dynamics of the heme, and its surrounding environment, play a critical role in the ability of myoglobin to reversibly bind oxygen and resist carbon monoxide binding (the latter is catastrophic, since CO binds irreversibly to the heme, making it inaccessible to O_2).

In this case study we will explore the structure and physical properties of myoglobin. The following files will be used:

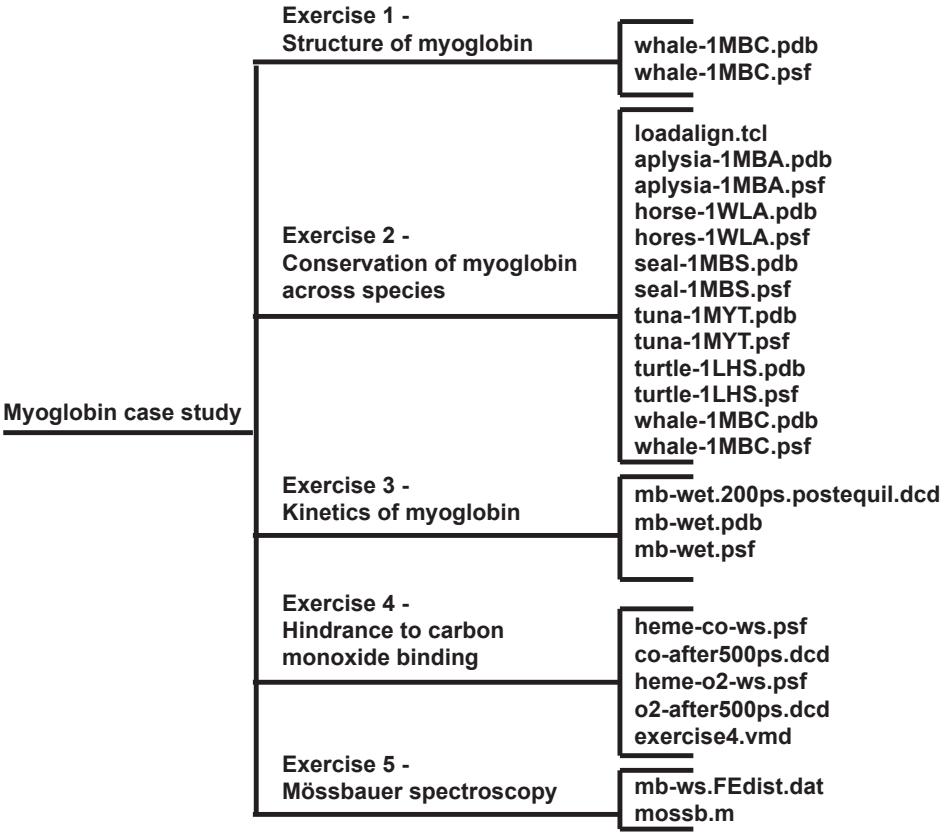

1 The structure of myoglobin

We first turn our attention to the structure and function of myogloblin, exploring its ubiquity and conservation across species, the means by which it reversibly binds oxygen, and the way in which it reduces carbon monoxide binding.

Myoglobin is a water-soluble globular protein of ~ 150 amino acids. The tertiary structure is composed of eight α-helices joined by short non-helical regions (Fig. 1). The helices provide a rigid structural framework for the heme pocket.

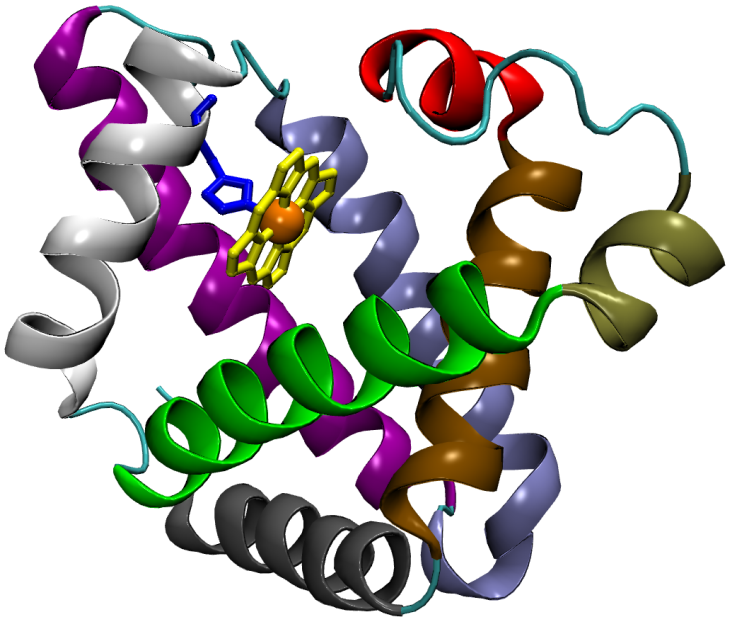

Figure 1: Myoglobin of sperm whale (*Physeter catodon*). The protein (whose structure is comprised of eight alpha-helices) is drawn in cartoon representation. The helices are distinguished by color. The heme group is shown in licorice representation bound to the histidine. The heme iron, drawn as an orange van der Waals sphere, is the binding site for ligands, such as O_2, CO and NO. The binding occurs at the distal (from the histidine) side of the heme, which is turned towards the viewer in this picture. [whale-1MBS.psf, whale-1MBS.pdb]

A heme group is bound in a hydrophobic cleft in the protein, and is key to the function of myoglobin: it is to the heme that oxygen binds. The heme itself consists of an organic ring known as protoporphyrin that surrounds an iron atom (Fig. 2a). The iron is ligated to

four nitrogens of the protoporphyrin, as well as to a histidine side-chain of myoglobin which tethers the heme in the hydrophobic pocket. This leaves a sixth ligation position, on the side of the heme plane opposite (distal) to the histidine, available for the binding of oxygen (Fig. 2b). Interactions with residues near the oxygen binding site serve to stabilize bound oxygen, as well as interfere with CO binding.

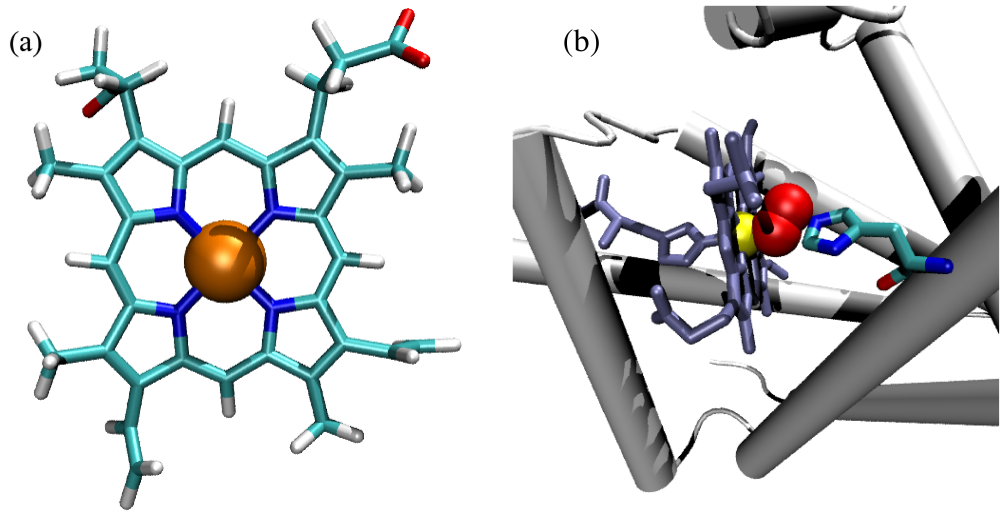

Figure 2: The heme group (a) and its binding environment in myoglobin (b). In (b), bound oxygen (O_2) is colored in red and the distal histidine, which influences the binding affinity, is shown colored by atom type; hydrogen atoms are not shown. The proximal histidine, which tethers the heme to the protein, is shown in the same shade of blue as the heme itself in (b). [whale-1MBS.psf, whale-1MBS.pdb]

The interior and exterior of myoglobin are well-distinguished by hydrophobic and hydrophilic side groups. Fig. 3 depicts the residues by hydrophobicity, and it is easily seen that the interior is made of hydrophobic (non-polar) side groups, whereas the exterior is made of hydrophilic (polar) side groups.

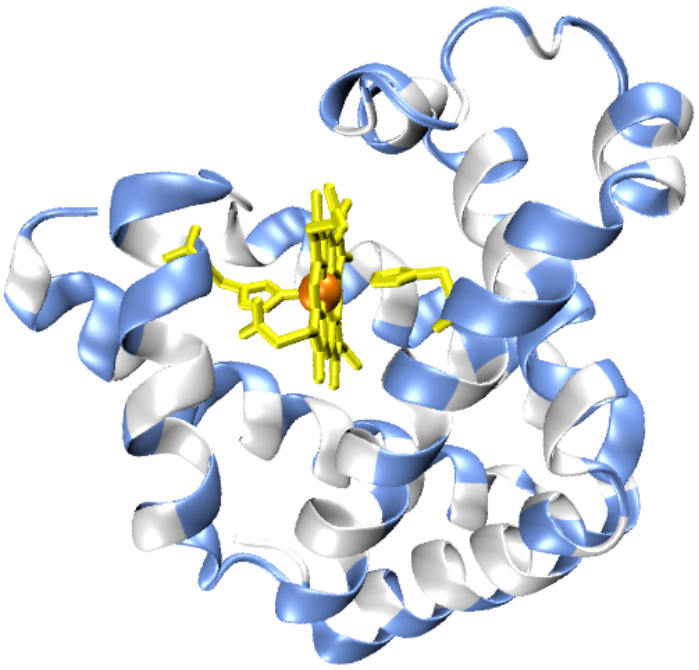

Figure 3: Heme (yellow, orange), proximal and distal histidines (yellow), and myoglobin backbone. For the backbone, hydrophobic residues are shown in white, and polar and charged residues are shown in blue. Residues on the interior of the protein are more likely to be hydrophobic. [whale-1MBS.psf, whale-1MBS.pdb]

Exercise 1: Structure of myoglobin.

Examine the crystal structure of sperm whale myoglobin in VMD by loading the psf file `whale-1MBC.psf` and coordinates file `whale-1MBC.pdb`.

- Find the heme and the proximal and distal histidines. What is the resid (residue number) for the proximal histidine? The distal histidine?
- Look at the protein in van der Walls and surface representations. Based on the static structure, do you consider this protein compact? Why or why not?
- Is a hydrophobic or polar environment better for O_2? Using van der Waals or surface representation, color the protein by residue type. Where do you suppose O_2 might enter myoglobin?

1.1 Myoglobin is ubiquitous and conserved across species

Figure 1 depicts the myoglobin of *Physeter catodon* (sperm whale). Because of the depths to which the sperm whale dives, its muscle tissue is rich in myoglobin; of the dozen myoglobin structures known today, it is that of the sperm whale which was first crystallized and has been the most extensively studied [14].

Today we have available resolved structures of myoglobins from species ranging from human to sea hare, *Aplysia limacina*, a mollusk that lives in shallow seawater. The structure of myoglobin is highly conserved across species. The overlapped structures of several myoglobins are shown in Fig. 4, colored by their sequence identity to sperm whale myogblobin.

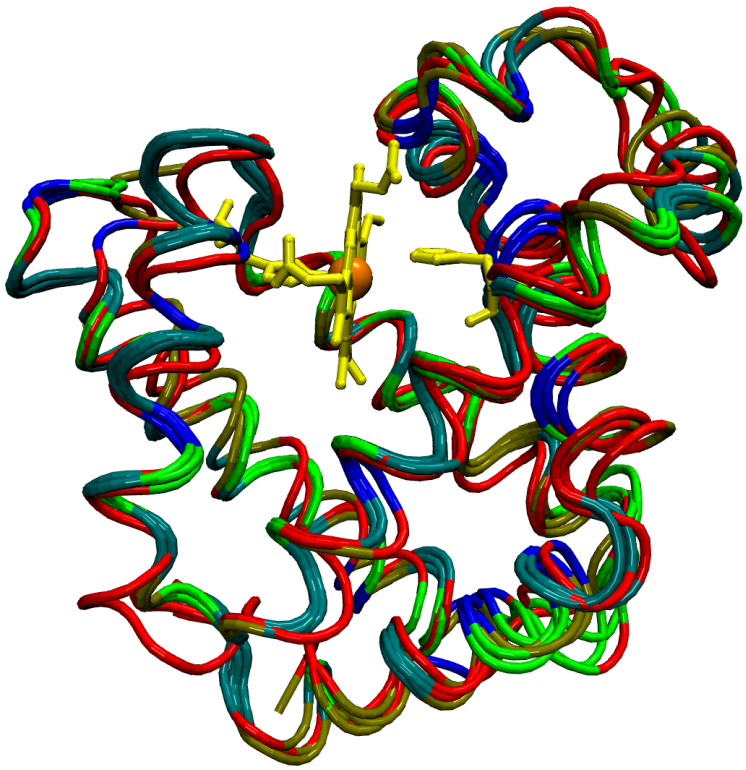

Figure 4: Myoglobins, aligned and colored by sequence identity to sperm whale myoglobin. The color scale indicates sequence conservation and ranges from highly identical, shown in blue, to complete lack of conservation, shown in red. The heme and adjacent histidines are shown in yellow for reference. Superimposed are the structures of whale, turtle, aplysia, tuna, and horse myoglobins.

Exercise 2: Conservation of myoglobin across species.

Load the structures of whale, turtle, aplysia, tuna, and horse myoglobin into VMD by typing `source loadalign.tcl` at the VMD prompt; this will run the script `loadalign.tcl`, which automatically loads the mentioned structures.

- Use the MultiSeq tool in VMD to align the structures and examine their sequence identity. Which sequences are most (least) similar to that of whale?
- Make a guess, based on what you know about myoglobin function, where in the structure you will find the most highly conserved residues. Do you find them where you expect? Do you find conserved residues elsewhere?
- You should have noticed that the aplysia sequence is considerably different from the other sequences. Where do the most significant differences lie?

1.2 Structure and kinetics of Mb aid in oxygen storage

The function of myoglobin, to serve as a temporary store of oxygen, requires that the heme environment is conducive not only to binding of oxygen, but also to doing so reversibly. In this regard, the bulk of the myoglobin molecule serves a two-fold purpose of modulating the heme environment to facilitate oxygenation as well as ensuring that the heme iron remains in a ferrous state. Heme groups that have been oxidized lose the ability to bind O_2. The oxidation goes through an intermediate in which O_2 is sandwiched between two hemes, and free hemes oxidize rapidly in blood. The myoglobin structure prevents this oxidation by sterically preventing a heme-O_2-heme complex.

Since the heme needs to be protected, the myoglobin is quite closely packed with amino acid side groups, and the heme is shielded to outside molecules, including to oxygen. But oxygen has to be delivered to the heme somehow. Indeed, one finds in myoglobin an interplay between shielding the heme and allowing oxygen in: the protein is packed densely to protect the heme, but there are certain places on the surface where O_2 can enter (see Fig. 5), and a limited number of pathways lead from the surface to the heme.

Interestingly, examination of a static structure of myoglobin, *i. e.* one obtained from the

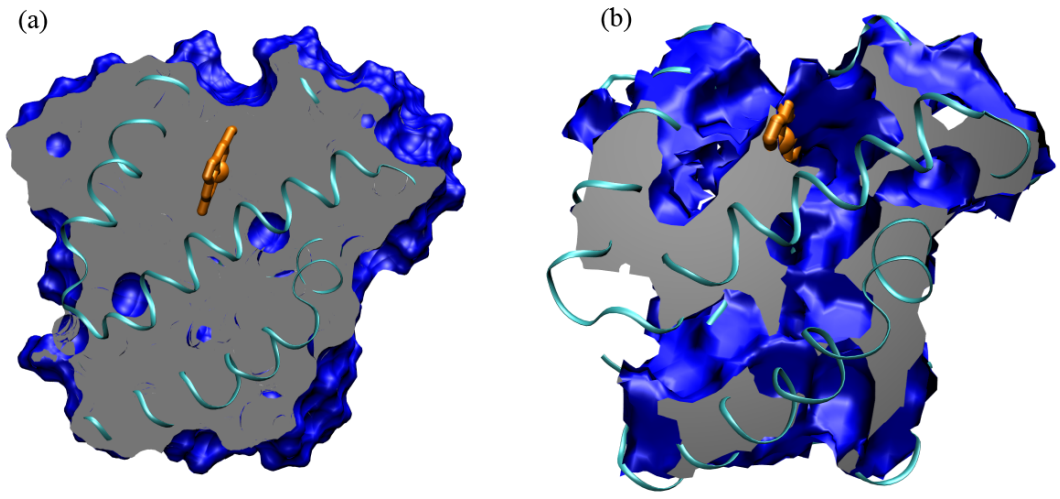

Figure 5: Accessibility to oxygen in the interior of the sperm whale myoglobin. A cut through the center of the protein (cutting plane is perpendicular to the heme) is shown. In (a), a static structure is examined. Cavities accessible to oxygen molecules and surface of the protein are shown in blue; the space not accessible to oxygen is colored in gray. In (b), the cavities arising due to the thermal motion of residues comprising the myoglobin are demonstrated. The heme is shown as a ring with the iron atom (big sphere) in the center.

crystallographic studies, shows no open pathways whatsoever (see Fig. 5a). The structure is very much closed, with only a small number of tiny cavities open, but disconnected. Then how can an oxygen molecule penetrate through to the heme group? To answer this question, one has to consider the dynamical properties of myoglobin. Myoglobin works at physiological temperatures of about 300 K at which it exhibits considerable thermal motion. It also exists in a highly dynamic environment of the cellular cytoplasm. What permits oxygen into myoglobin are fluctuations of its structure, inevitable under the thermal conditions under which myoglobin performs its function. Due to the thermal fluctuations of the residues comprising the protein, there is a possibility for the structure to have random cavities where oxygen molecules can fit in. The random cavities are spreading throughout the protein, and O_2 molecules can travel along with these openings. As a result, the interior of myoglobin, statically apparently closed to oxygen, is dynamically actually open. This is demonstrated dramatically in Fig. 5b. However, due to the probabilistic nature of the fluctuations that allow for oxygen migration inside myoglobin, it is not straightforward for O_2 to reach the

heme. An oxygen molecule is moving through the randomly opening cavities until it accidentally approaches the heme, a process which is very long (ns to μs) in comparison with the time scale of local movements of the protein residues (ps).

The wide channels shown in Fig. 5b should not be taken literally. The picture only shows where oxygen can go in principle, considering a very long (μs) time scale (this picture was produced in a computer simulation of myoglobin dynamics, as described in [15]). At each moment, the myoglobin interior (in terms of the accessibility to O_2) looks like the image in Fig. 5a, rather the one in Fig. 5b. The random opening and migration of the small cavities over a course of long dynamics, arising due to the flexibility of the protein, make it possible for O_2 to explore a substantial part of myoglobin's interior and to reach the heme. That is why one does not talk about oxygen channels in myoglobin (there are no real structural channels); instead, the term "pathway" is used.

The widest pathway found Fig. 5b is the going straight from the heme to the surface; it is also the shortest way from the heme to the outside. This is the so-called distal oxygen pathway. If, in addition to the geometrical considerations, the energy of interaction between the residues of the myoglobin and O_2 is taken into account, the distal pathway also appears to have a larger affinity to oxygen than most other parts of the protein. Being very short and relatively favorable for oxygen, the distal pathway might well be the main transport root in the oxygen exchange between the heme and outside medium (in addition to binding oxygen effectively, it is also important for the myoglobin to release O_2 effectively, when the latter is needed in for the surrounding cellular machinery). The probabilistic pathways together with the tight packing make myoglobin's oxygen storage and transduction highly reliable.

Exercise 3: Kinetics of myoglobin.

Load the structure of sperm whale myoglobin structure `mb-wet.psf` and the short trajectory `mb-wet.200ps.postequil.dcd` into VMD.

- Compare the structures to the pockets you see in Figure 5b. What do you notice about the residues near the openings in the myoglobin? Does this image agree or disagree with your hypothesis for O_2 entry into myoglobin?
- Examine the RMSD per residue for the protein side chains using the trajectory you loaded. How does this compare to the channels depicted in Figure 5b?

1.3 How the Mb structure hinders carbon monoxide binding

The heme environment in myoglobin confers some protection against carbon monoxide poisoning. Because heme naturally binds CO $25,000$-times more strongly than it binds O_2, carbon monoxide asphyxiates cells from within by blocking oxygen uptake (cyanide poisoning occurs in a similar fashion, binding to the heme of the electron transport protein cytochrome c). However, the so-called distal histidine of myoglobin, on the oxygen-binding heme face, forces CO (and O_2) to bind at an angle to the heme, and is believed to be responsible for reducing by two orders of magnitude the affinity for CO [14]. While O_2 readily takes the conformation enforced by the distal histidine, CO does not; the difference can be clearly seen from simple MD calculations.

To examine the preferred binding angle of ligands to the heme, two simulations are conducted: each one of a heme in water sphere with a base on the proximal side (in this case, as in myoglobin, histidine) and either CO or O_2 bound on the distal side. The $\mathrm{Fe}-\mathrm{C}-\mathrm{O}$ (for CO) and $\mathrm{Fe}-\mathrm{O}-\mathrm{O}$ (for O_2) angles are then plotted over time after an initial 1 ns equilibration period.

The results (Fig. 6) of the unenclosed heme simulations are revealing. The bound CO remains bound at a near-straight 173^o angle. The fluctuations from this favored configuration are slight; indeed, the root mean squared deviation (RMSD) from this angle is only 3^o, and we gather that the preferred configuration is relatively stable even at temperatures of 310 K. In contrast, the preferred O_2 binding angle is shallower, averaging 156^o. More importantly, the

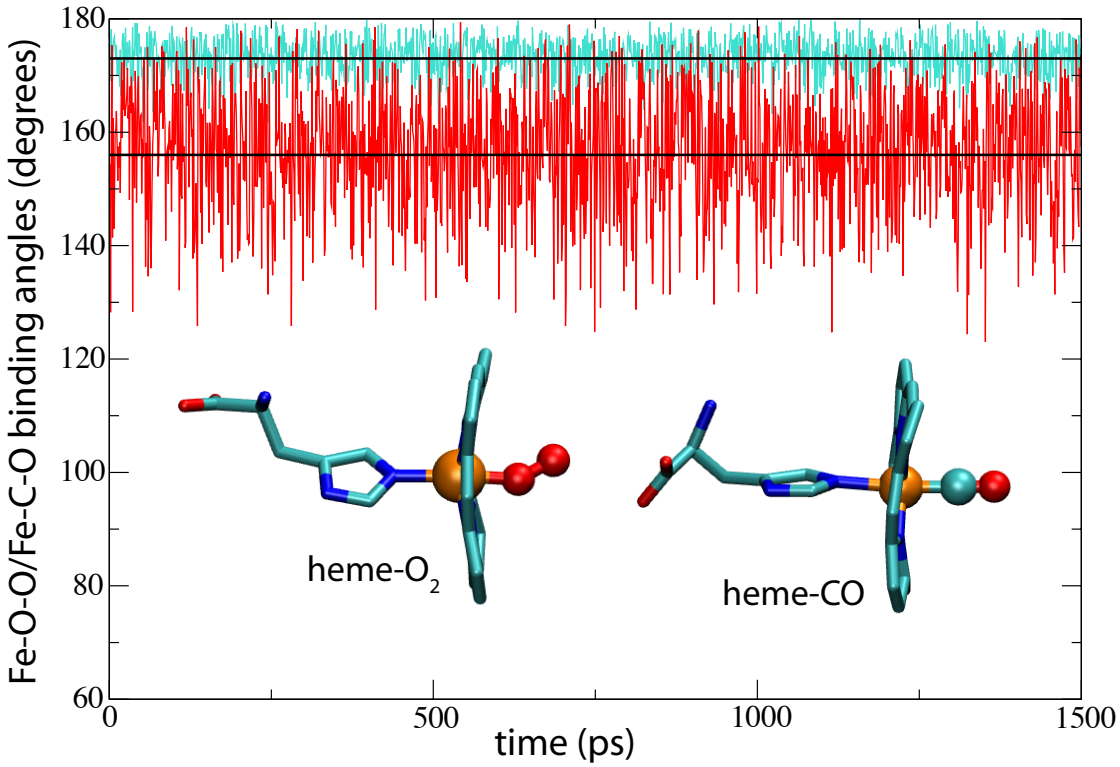

Figure 6: Plots of Fe-C-O angle (cyan) and Fe-O-O angle (red). The averages for both plots are shown in black. The insets depict the simulated systems (water, ions, hydrogens, and non-plane heme atoms are not shown). The O_2 binding angle is noticeably smaller and more flexible.

RMSD fluctuation of the O_2 binding angle is much greater than that of the similarly-massive CO by 12^o.

Exercise 4: Hindrance to CO binding in myoglobin.

- Open VMD and load the saved state Exe4/exercise4.vmd. Play the trajectory for both heme-CO and heme-O2. What is the difference of the CO binding and O2 binding? Orient the molecules so that the difference can be seen clearly and render pictures of heme similar to fig. 6.
- Chose the VMD menu Mouse → Label → Angles. Select the atoms that form the binding angles (Fe-C-O for CO, and Fe-O-O for O_2). Use VMD menu Graphics → Labels to plot the binding angles over time. Compare the plots with Fig. 6.
- What do the comparative flexibilities of the binding angles for O_2 and CO suggest to you about the energetic cost associated with enforcing a shallow binding angle?
- Recall the structures and sequences you loaded previously. How do the residues near the binding site compare across species? What might you hypothesize about the function of aplysia myoglobin?

2 Mössbauer spectroscopy*

To study the function of a protein it is often very important to investigate the protein's dynamics. As we saw above, the myoglobin's ability to store oxygen depends crucially on the thermal motion of amino acids this protein consists of. Unfortunately, there are not many experimental techniques that allow one to study internal motions in a protein in the native environment, non-invasively, and with high time resolution. For example, x-ray crystallography or NMR spectroscopy can give invaluable information about protein's structure, but they are usually not suitable to study the dynamics of the protein. However, sometimes it is possible to investigate the motion of parts of a protein using the so-called Mössbauer spectroscopy. In particular, the dynamics of myoglobin's heme group can be studied using this method.

The Mössbauer spectroscopy uses high-energy photons ($10^4 - 10^6$ eV, *i. e.* gamma-rays) to probe the samples containing the molecules being studied. The sample is irradiated with the photons of specific energy, tuned to match the transitions between energy levels in

certain nuclei. On absorbing a photon, the nucleus becomes excited. Then a spontaneous transition to the ground state occurs, and the nucleus emits a photon. Detecting the photons re-emitted by the sample and analyzing their spectrum, it is possible (as shown below) to extract the information about the motion of the nuclei between the absorption and re-emission of the photon. Since the gamma-rays have the wavelength of ~ 1 Å and below, the spatial resolution of the Mössbauer spectroscopy corresponds very well to the interatomic distances in the biomolecules (which usually is of the order of few Å).

There is, however, a problem with applying the Mössbauer spectroscopy to an arbitrary system. The excitations in nuclei of most atoms comprising the biomolecules have very short life times, of the order of 10^{-17} s, while the motions of interest in biomolecular systems occur on a time scale of $10^{-12} - 10^{-6}$ s and beyond. A typical nucleus re-emits a photon with a time delay negligible for any practical purpose, and no information about the nucleus' motion can be extracted, because between the absorption and emission the nucleus practically remains at rest. If the exposure of biological systems to gamma-rays would be non-invasive, one could use a high intensity irradiation to obtain a high temporal resolution (10^{-17} s) studying the natural motion of the nuclei. But the energies of gamma-quanta are so huge ($10^4 - 10^6$ eV corresponds to $10^8 - 10^{10}$ K), that only very small irradiation intensities can be used; otherwise, very fast the system would be completely destroyed by the gamma-rays. Due to these difficulties, the applications of the Mössbauer spectroscopy in biological experiments is restricted to a very weak irradiation and to a work with a limited list of nuclei for which the excitation life time is large enough.

One of the nuclei with a long excitation life time is ^{57}Fe. This is the nucleus which is situated in the center of the myoglobin's heme group, and therefore the myoglobin is suitable for studies involving the Mössbauer spectroscopy. The excitation life time τ of ^{57}Fe is 10^{-7} s, corresponding to the characteristic times ($10^{-9} - 10^{-7}$ s) of the motion of the heme group and amino acids comprising the myoglobin. To appreciate how exceptional the transition in ^{57}Fe is, one should note that the re-emission of the gamma-quantum by the nucleus is a probabilistic process, whose life time is connected with the so-called natural spectral line width Γ by the uncertainty principle,

$$\Delta E \Delta t = \Gamma \tau \simeq \hbar \tag{1}$$

The excitation life time $\tau = 10^{-7}$ s corresponds to a very narrow natural line width, $5{\cdot}10^{-9}$ eV (by contrast, the emitted photon has an energy of 14.4 keV).

The Brownian motion of the heme iron in the myoglobin can be probed by examining the Mössbauer spectrum line shape; in fact, many experimental and theoretical studies have examined the Mössbauer effect in globular proteins (e.g., [16, 17, 18]). Conversely, given known ^{57}Fe motion from a computer simulation, it is possible to predict the Mössbauer line shape $I(\omega)$. In the following example we obtain the Mössbauer line shape $I(\omega)$ for the motion of the heme's iron in the sperm whale myoglobin.

The Mössbauer spectrum $I(\omega)$ is given by the following expression (as shown in [19, 20, 21]):

$$I(\omega) = \frac{\sigma_0 \Gamma}{2} \int_{-\infty}^{\infty} dt \exp\left[-i\omega t - \frac{\Gamma|t-t_0|}{2\hbar}\right] G(\vec{k}, t, t_0), \tag{2}$$

where Γ is the natural line width ($\Gamma/\hbar = 7 \cdot 10^{-6}\mathrm{s}^{-1}$) and $G(\vec{k}, t, t_0)$ is given by

$$G(\vec{k}, t, t_0) = \int dr \int dr_0 \exp\left[i\vec{k} \cdot (\vec{r} - \vec{r_0})\right] p(\vec{r}, t|\vec{r_0}, t_0) p_0(\vec{r_0})\,. \tag{3}$$

Here, $\vec{k}$ is the scattering vector of the gamma-ray, $\vec{r}$ is the position of the ^{57}Fe nucleus, $p(\vec{r}, t|\vec{r_0}, t_0)$ denotes the probability that ^{57}Fe is at position $\vec{r}$ at time t given an initial position of $\vec{r_0}$ at time t_0, and $p_0(\vec{r_0})$ is the probability to find ^{57}Fe at position $\vec{r_0}$ at time t_0. $G(\vec{k}, t, t_0)$ is thus just the autocorrelation function of $\exp[-i\vec{k}\cdot(\vec{r}(t)-\vec{r}(t_0))]$, *i.e.*, $G(\vec{k}, t, t_0) = \langle \exp[\vec{k}\cdot(\vec{r}(t)-\vec{r}(t_0))]\rangle$ where $\langle ...\rangle$ denotes the average over all initial positions $\vec{r}(t_0)$ and over all trajectories ending in $\vec{r}(t)$. For an estimate, take the momentum $|\vec{k}|$ of the gamma quantum to be 7.3 Å^{-1} [19], and the resonance absorption cross section $\sigma_0 = 0.015$ Å^2 [22].

The iron atom is tightly ligated in the center of the myoglobin's heme, so that the motion of ^{57}Fe studied by the means of Mössbauer spectroscopy is determined by the motion of the heme relative to the rest of the myoglobin. For this study, a simulation of the sperm whale myoglobin (`whale-1MBC.pdb, whale-1MBC.psf`) without oxygen bound to the heme was performed (at the temperature $T = 300$ K). The displacement of the iron perpendicular to the plane of the heme was monitored over the course of 2 ns as shown in Fig. 7.

The displacement of the heme's ^{57}Fe exhibits a standard deviation $\delta = 0.068$ Å and mean value $a = -0.017$ Å, slightly outside the plane of the heme. The displacement distribution can be found in Fig. 8 and is reproduced well by a Gaussian, *i.e.*, by the Boltzmann distri-

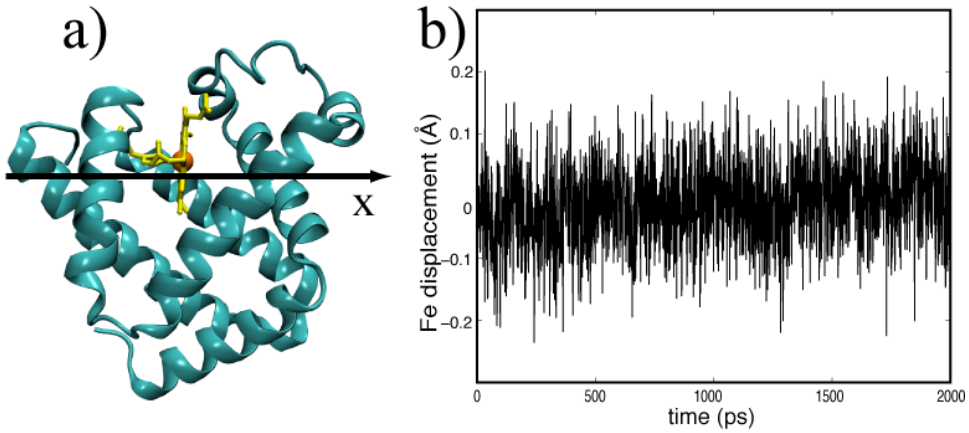

Figure 7: Displacement of the heme's iron atom. In (a), the analyzed direction of ^{57}Fe motion is denoted as x axis. In (b), the displacement of the heme's iron atom relative to the myoglobin as a whole over 2 ns is plotted as a function of time.

bution of a particle in a harmonic oscillator potential well. For our analysis, we therefore assume that ^{57}Fe, which is attached (Fig. 2a) to the myoglobin's heme, is in a harmonic well potential. The spring constant f that best matches the Gaussian in Fig. 8 to the distribution extracted from the simulation is $f = k_B T/\delta^2 = 8.9 \cdot 10^3$ pN/Å (k_B is the Boltzmann's constant).

For an approximate analysis, assume that ^{57}Fe is a Brownian particle of mass m moving in one-dimensional space in a potential $U(x)$; also, set $t_0 = 0$. Dynamics of the particle is governed by the Langevin equation

$$m\ddot{x} = -\frac{d}{dx}U - \gamma\dot{x} + \chi(t) \tag{4}$$

where γ represents the friction constant and $\chi(t)$ is the Gaussian white noise. For the harmonic potential $U(x) = fx^2/2$ (centered at the equilibrium position of ^{57}Fe) this can be written

$$\ddot{x} + b\dot{x} + \omega_0^2 x = \eta(t) \tag{5}$$

where $b = \gamma/m$, $\omega_0^2 = f/m$ and $\eta(t) = \chi(t)/m$. According to the expression (2), the Mössbauer lineshape $I(\omega)$ is the Fourier transform of the position autocorrelation function. The expression for this function can be derived analytically for the motion of a Brownian

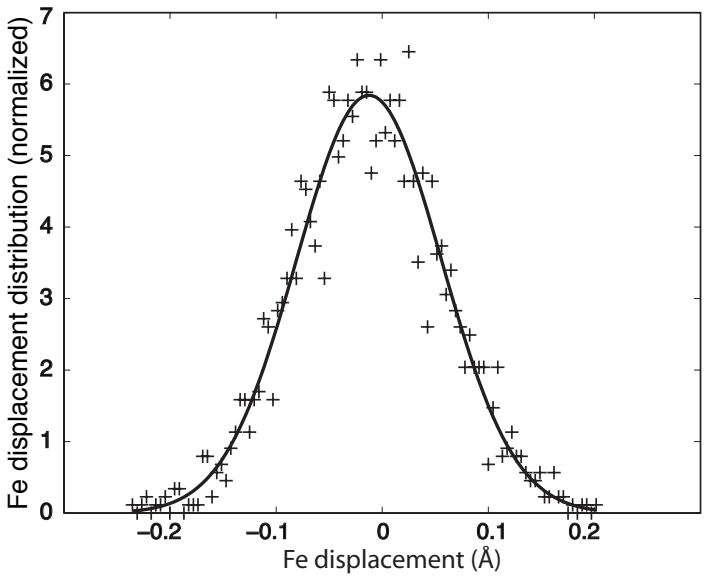

Figure 8: Distribution of displacements of ^{57}Fe. The data extracted from the simulation is shown as pluses; a Gaussian fit to the data is shown as a solid black line.

particle in an overdamped oscillator ($b >> \omega_0$ in Eq. 5) and is given by

$$\langle x(0)x(t)\rangle = \exp(-b|t|/2)\left[\cosh(\omega_0 t) + \frac{b}{2\omega_0}\sinh(\omega_0 t)\right] . \tag{6}$$

The position autocorrelation function $< x(t)x(0) >$ can also be determined from the computer simulation. The resulting autocorrelation function is plotted in Fig. 9.

After calculating the autocorrelation function from the simulation, one can match the result to the analytical expression in Eq. 6 and thus determine γ, the only unknown constant. From the fit in Fig. 9 one obtains $\gamma = 1.96 \cdot 10^6$ pN $\cdot$ ps/Å. The damping coefficient γ in the Langevin equation 4 is connected with the diffusion coefficient D by the expression $D = k_B T/\gamma$; using $T = 300$ K, we obtain $D \approx 2 \times 10^{-2}$ Å^2/ns.

Following the algebra in [21], it can be shown that for an overdamped harmonic oscillator (Eq. 5), the Mössbauer spectrum $I(\omega)$ has the form

$$I(\omega) = \frac{\sigma_0 \Gamma}{2}\int_{-\infty}^{\infty} dt \exp\left[-i\omega t - \frac{\Gamma|t|}{2\hbar} - \frac{k_B T k^2}{\alpha\gamma}(1 - e^{(-\alpha|t|)})\right] , \tag{7}$$

where $\alpha = \omega_0^2/b = f/\gamma$. Since the integral in $I(\omega)$ (Eq. 7) is the Fourier transform of

$$\exp\left(-\frac{1}{2}\Gamma|t| - \frac{k_B T k^2}{\alpha\gamma}(1 - e^{-\alpha|t|})\right) , \tag{8}$$

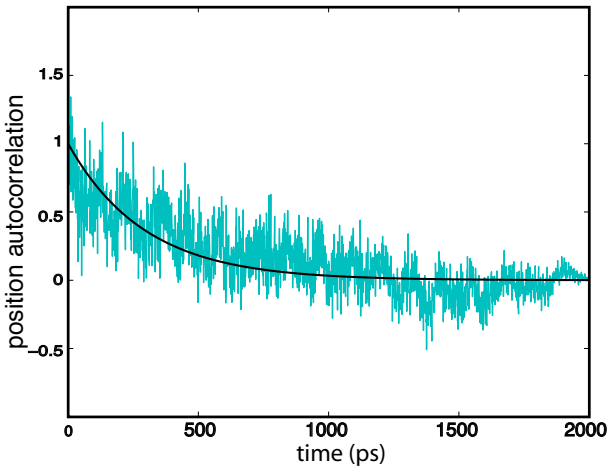

Figure 9: Position autocorrelation function data (cyan) and fit (solid black line) for the Fe displacement in the myoglobin over 2 ns.

one can use the values determined for γ and f to obtain the expected form of $I(\omega)$. The result is shown in Fig. 10.

We have seen that a computer simulation of the ^{57}Fe motion in the myoglobin enables one to calculate the diffusion coefficient for ^{57}Fe and predict the Mössbauer lineshape. Inverse procedure is possible in the analysis of the experimental data. From the experiment one extracts the Mössbauer lineshape $I(\omega)$, like the one in Fig. 10. Applying the inverse Fourier transform to $I(\omega)$, one gets the position autocorrelation function for ^{57}Fe, like the one in Fig. 9. Then the expression for the autocorrelation function, like the one in Eq. 6 (the actual expression may vary, depending on the approximations and model being used), is fitted to the experimental autocorrelation function. The best fitting gives the parameters that describe the motion of ^{57}Fe, on the time scale of nanoseconds. For example, one could fit the expression (6) to a hypothetical experimental autocorrelation function varying the parameters b and ω_0. The best fitting would therefore provide the 'experimental' values for $\gamma = bm$ and $f = m\omega_0^2$, the damping coefficient in the Langevin equation (4) and the oscillator's force constant, respectively; having γ, one also obtains the diffusion coefficient $D = k_B T/\gamma$. This shows that the Mössbauer spectroscopy can be used for the myoglobin to characterize, for example, the forces exerted by the environment on the heme's iron atom and to investigate the conditions in which the iron atom moves. Utilizing the Mössbauer

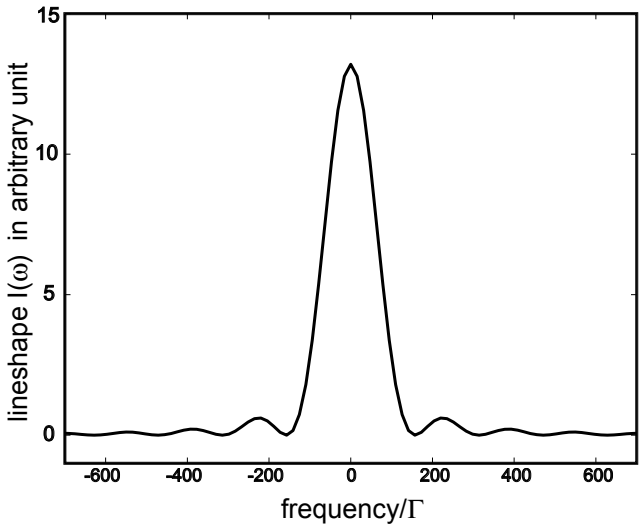

Figure 10: Mössbauer line shape function $I(\omega)$ in arbitrary units as a function of multiples of the natural line width Γ. The curve is the solution of Eq. 7 given $\gamma = 1.96 \cdot 10^6$ pN $\cdot$ ps/Å and $f = 8.9 \cdot 10^3$ pN/Å.

spectroscopy, one therefore probes the internal motions in the protein at an essential time scale, which helps to study the modes of operation and function of the protein.

Exercise 5: Mössbauer spectroscopy.

- The file *mb-ws.FEdist.dat* provides the ^{57}Fe displacements in myoglobin, measured in in Å with the time step of 1 ps at temperature T = 300 K. Interested readers are encouraged to analyze the data and obtain the Mössbauer spectrum by themselves using any mathematical software. A Matlab script for such analysis is provided in the file `moss.m`.

References

[1] J. C. Kendrew, R. E. Dickerson, B. E. Strandberg, R. G. Hart, D. R. Davies, D. C. Phillips, and V. C. Shore. Structure of myoglobin: A three-dimensional fourier synthesis at 2 angstrom resolution. *Nature*, 185:422–427, 1960.

[2] M. F. Perutz, M. G. Rossmann, A. F. Cullis, H. Muirhead, G . Will, and A. C. T. North. Structure of myoglobin: A three-dimensional fourier synthesis at 5.5 angstrom resolution, obtained by x-ray analysis. *Nature*, 185:416–422, 1960.

[3] A. Deriu. The power of quasielectric neutron scattering to probe biophysical systems. *Physica B*, 182(4):349–360, December 1992.

[4] Martin Karplus. Molecular dynamics: Applications to proteins. In J.-L. Rivail, editor, *Modelling of Molecular Structures and Properties*, volume 71 of *Studies in Physical and Theoretical Chemistry*, pages 427–461, Amsterdam, 1990. Elsevier Science Publishers. Proceedings of an International Meeting.

[5] Richard J. Loncharich and Bernard R. Brooks. Temperature dependence of dynamics of hydrated myoglobin. *J. Mol. Biol.*, 215:439–455, 1990.

[6] J. Smith, K. Kuczera, and M. Karplus. Dynamics of myoglobin: Comparison of simulation results with neutron scattering spectra. *Proc. Natl. Acad. Sci. USA*, 87:1601–1605, 1990.

[7] Jeung Sun Ahn, Yasuo Kanematsu, Makoto Enomoto, and Takashi Kushida. Determination of weighted density states of vibrational modes in Zn-substituted myoglobin. *Chem. Phys. Lett.*, 215:336–340, 1993.

[8] E.R. Henry, W.R. Eaton, and R.M. Hochstrasser. Molecular dynamics simulations of cooling in laser-excited heme proteins. *Proc. Natl. Acad. Sci. USA*, 83:8982–8986, 1986.

[9] S. Cusack and W. Doster. Temperature dependence of the low frequency dynamics of myoglobin – measurement of the vibrational frequency distribution by inelastic neutron scattering. *Biophys. J.*, 58:243–251, 1990.

[10] J. D. Hirst and C. L. Brooks. Molecular dynamics simulations of isolated helices of myoglobin. *Biochemistry*, 34(23):7614–7621, June 1995.

[11] Cecilia Bossa, Massimiliano Anselmi, Danilo Roccatano, Andrea Amadei, Beatrice Vallone, Maurizio Brunori, and Alfredo Di Nola. Extended molecular dynamics simulation of the carbon monoxide migration in sperm whale myoglobin. *Biophys. J.*, 86:3855–3862, 2004.

[12] Maurizio Brunori and Quentin H. Gibson. Cavities and packing defects in the structural dynamics of myoglobin. *EMBO Rep.*, 2(8):676–679, 2001.

[13] M. Brunori, D. Bourgeois, and B. Vallone. The structural dynamics of myoglobin. *J. Struct. Biol.*, 147:223–234, 2004.

[14] L. Stryer. *Biochemistry*. W. H. Freeman and Co., New York, 4th edition, 1995.

[15] Jordi Cohen, Kwiseon Kim, Paul King, Michael Seibert, and Klaus Schulten. Finding gas diffusion pathways in proteins: Application to O_2 and H_2 transport in CpI [FeFe]-hydrogenase and the role of packing defects. *Structure*, 13:1321–1329, 2005.

[16] V. Lisy, T. Yu. Tchesskaya, and A. V. Zatovskii. A simple theory of the spectra of absorption and rayleigh scattering of Mössbauer radiation by globular macromolecules. In *Spectroscopy of Biological Molecules: Modern Trends*, pages 581–582. Kluwer Academic Publishers, 1997.

[17] A. V. Zatovskii, V. Lisy, and T. Yu. Tchesskaya. Effect of moisture content of globular proteins on the parameters of Mössbauer spectra. *Optics and Spectroscopy*, 84:201–206, 1998.

[18] T. Yu. Chesskaya. Dynamics of globular molecules: the effect of mixture content on the rayleigh scattering spectrum of Mössbauer radiation. *Chemical Physics Reports*, 17:1975–1986, 1998.

[19] Walter Nadler and Klaus Schulten. Generalized moment expansion for the Mössbauer spectrum of Brownian particles. *Phys. Rev. Lett.*, 51:1712–1715, 1983.

[20] Walter Nadler and Klaus Schulten. Theory of Mössbauer spectra of proteins fluctuating between conformational substates. *Proc. Natl. Acad. Sci. USA*, 81:5719–5723, 1984.

[21] R. Nowik, E. R. Bauminger, S. G. Cohen, and S. Ofer. Spectral shapes of Mössbauer absorption and incoherent neutron scattering from harmonically bound nuclei in Brownian motion. *Physical Review A*, 31:2291–2299, 1985.

[22] A. C. Melissinos. *Experiments in Modern Physics.* Academic Press, Inc., 1966.